Available online at www.sciencedirect.com
SCIENCE DIRECT®
Journal of Crystal Growth 275 (2005) 83–90
JOURNAL OF CRYSTAL GROWTH
www.elsevier.com/locate/jcrysgro

Local order in interfaces

J.P.J.M. van der Eerden*, J. Makkinje, T.J.H. Vlugt

Condensed Matter and Interfaces, Debye Institute, Utrecht University P.O. Box 80.000, 3508 TA Utrecht, The Netherlands

Available online 15 December 2004

Abstract

In this paper we discuss the state of the art of describing the structure and dynamics of crystal surfaces at the atomic level. Depending on the type of processes that one wants to describe, different approaches are to be chosen. We focus on equilibrium surface structures at the scale of typical growth units during growth or melting. For atomic crystals these length scales are Angstroms, for nano-crystals and organic molecules, nanometres, for colloids and proteins up to 10–100 nm.

The challenge is to find a reliable description of a growth unit and its environment that is computationally cheap, informative and involves as little neighbouring growth units as possible. We explain how the environment of a growth unit can be defined, how we found optimal local order parameters, and we discuss some published and some new results. Our discussion is based on molecular simulation, mostly of Lennard-Jones crystals.

PACS: 07.05.T; 61.16.C; 81.10.A; 68.35.M

Keywords: Computer simulation; Surface structure; Nucleation; Growth models

1. Introduction

Crystal growth is an intricate interplay of processes at different length and time scales. Nevertheless the region where atoms or molecules change from 'mother phase like' to 'crystal like' extends over a few molecular layers only. This is caused by the fact that crystallization is a first-order phase transition. At thermodynamic equilibrium mother phase and crystal phase coexist, with distinctly different thermodynamic properties, e.g. density, molar energy, compressibility and heat capacity are different in the two phases. X-ray diffraction is used to analyse the corresponding differences on atomic scales.

It costs free energy to perturb either of these phases. When two phases are in contact, the length scale at each phase will be modified, which is its correlation length ξ. For crystals and liquids, the correlation length is usually a few molecular distances, which is therefore the typical

*Corresponding author. Tel.: +31 30 253 3125; fax: +31 30 2532403.
E-mail address: j.p.j.m.vandereerden@chem.uu.nl (J.P.J.M. van der Eerden).

0022-0248/$ - see front matter © 2004 Elsevier B.V. All rights reserved.
doi:10.1016/j.jcrysgro.2004.10.070

equilibrium interface thickness. Experimentally this hinders easy access to structural and dynamical interface properties. Only recently strong X-ray sources, combined with elaborate numerical interpretation software, give access to crystal–solution interfaces with molecular resolution. Also scanning probe microscopy can, in some cases, observe crystal surfaces with molecular resolution.

Despite the difficulty to access surfaces with high resolution, the structural changes at the molecular level are at the heart of the crystal growth process. Though macroscopic, slowly evolving structures have a decisive influence on the net crystal growth rate and the final crystal quality, the underlying atomic-scale processes set up the scene.

In this paper we focus on the atomic-scale. Atomic-scale structures and processes have various macroscopic consequences. The strength of the atomic-scale interaction determines which macroscopic phase is stable at a given temperature. Atomic-scale interactions and structures determine a relevant correlation length ξ, which in turn, determines the local interface width. Though there is no solid–liquid critical point, critical points, where $\xi \to \infty$, are often important in crystal growth. An example is the growth of protein crystals, where it has been shown that optimum nucleation conditions are found when the salt and protein concentrations are close to the critical point of dense and dilute protein solutions. Above the roughening temperature, the crystal surface is critical, the edge free energy is zero and the correlation length ξ is infinite. Macroscopically atomic-scale roughening implies rounding of a crystal surface. Further interplay between atomic-scale and macroscopic structure is found in growth forms, e.g. molecular diffusion and local growth rate lead to a diffusion length scale that determines whether the macroscopic crystal shape is convex, dendritic or fractal.

Throughout the paper we use the words 'growth unit' for the stoichiometric set of atoms, ions or molecules that build up the crystal. We discuss sensible definitions of the neighbourhood $\Omega(i)$ of growth unit i. Bond order parameters are introduced to characterize $\Omega(i)$. We give criteria for the quality of an order parameter. We use Monte Carlo simulations of Lennard-Jones systems to test a large number of order parameters and with the best ones we characterize interfaces.

2. Local structure in lattice models

The simplest lattice model for crystal growth is the Kossel [1] model, a simple cubic lattice where on each lattice position, a growth unit may or may not be present. The model was put forward by Stranski and Kaischew [2] and further employed by Burton et al. [3] to explain why some crystals have natural faces, whereas others do not. Nowadays almost arbitrary lattices can be used routinely. The structure of the mother phase is taken into account only in an average, mean field sense.

Studies of lattice models have been a rich source of inspiration for developing general insight into surface structure, surface roughening and crystal morphology. It became clear that systems for which the surfaces have energetic preference for discrete positions along their normal axis have a thermodynamically well-defined surface phase transition, called the roughening transition [4]. Below the transition temperature, the surface is atomically smooth, the crystal develops facets and grows with step mechanisms [5]. Above that temperature, the surface is atomically rough, the crystal face becomes macroscopically curved, and it grows linearly with supersaturation. Below the roughening point, the most pregnant impurity effect is the formation of macrosteps via step bunching. Above the roughening point, morphological instability is usually the most important effect.

Surfaces that are parallel to strong bond directions have a high roughening temperature and grow slowly. The Hartman–Perdok theory analyses the crystal graph (the bond structure on the crystal lattice) to find slow-growing orientations. When the crystal unit cell contains more than one growth unit, the analysis of the crystal graph and the estimation of the net crystal growth rate are very complex. The crystal graph analysis and the calculation of the growth rate are being automated [6,7] to make the basic ideas usable on

a routine basis. The predictive power of this approach is satisfactory in many cases.

3. Continuum model for growth from dense phases

The local (in the sense of atomic-scale neighbourhood) surface structure determines the macroscopic crystal shape and crystal growth rate. This forms the general motivation to study crystal growth processes on an atomic-scale. A problem is that growth units do not stay at ideal lattice positions, especially for growth from concentrated solutions or from melts, lattice models are inadequate.

The best-known off-lattice model is the Lennard-Jones model. It possesses a stable hexagonally close-packed (HCP) crystal phase, a liquid phase and a gas phase. It is the generic model for crystal growth from the melt and it can be used for growth from the vapour as well. The potential energy depends on the particle positions $\mathbf{r}^N$. It is built up from isotropic pair potentials, which are strongly repulsive at short distance, attractive at intermediate distance and negligible at large distance:

$$E_{\mathrm{pot}}(\mathbf{r}^N) = \sum_{i=1}^{N-1} \sum_{j=i+1}^{N} V(|\mathbf{r}_i - \mathbf{r}_j|), \tag{1}$$

$$V(r) = 4\varepsilon \left[\left(\frac{\sigma}{r}\right)^{12} - \left(\frac{\sigma}{r}\right)^{6} \right] f^{\mathrm{co}}\left(\frac{r}{r^{\mathrm{co}}}\right). \tag{2}$$

Here f^{co} is a smooth cut-off function ($f^{\mathrm{co}} = 0$ for $r > r^{\mathrm{co}} \approx 2.5\sigma$), $\varepsilon/k_{\mathrm{B}} = 114.1\,\mathrm{K}$ is the bond energy and $\sigma = 0.3405\,\mathrm{nm}$ the atom diameter.

In the Lennard-Jones model crystal growth and nucleation from the melt have been simulated. Below the melting point, the HCP phase is only slightly more stable than face centered cubic (FCC), whence in simulation experiments often randomly stacked layers (RCP) are found rather than the stable phase. Using straightforward MC or MD, these processes can be studied only under conditions that are, from an experimental point of view exotic. Indeed growth rates of the order of $1\,\mathrm{m/s}$ and nucleation rates of the order of $10^{25}\,\mathrm{s}^{-1}\,\mathrm{mm}^{-3}$ were accessible [8].

Some of the results of these simulations were in line with the theory developed for the lattice models. Indeed the dimensionless heat of melting $\Delta H_{\mathrm{m}}/(k_{\mathrm{B}}T_{\mathrm{m}}) \approx 1.8$ is so small that all crystal–melt surfaces were expected to be rough. Indeed, the growth rate R depended linearly on the undercooling $\Delta T = T_{\mathrm{m}} - T$ over a large undercooling range and the crystal–melt surface tension was nearly isotropic [9–14]. Also the classical nucleation theory, if properly parameterized, described the dependence of the nucleation rate on the heat of melting and undercooling [15,16] and pressure [17] quite well.

Other results, however, were surprising. The growth rate anisotropy, i.e. the dependence of the growth rate R on the surface orientation (hkl) was much stronger than expected and the observed order $R(1\,1\,1) < R(1\,1\,0) < R(1\,0\,0)$ in the simulations was different from the lattice prediction $R(1\,1\,1) < R(1\,0\,0) < R(1\,1\,0)$. Careful studies on the structure of a Lennard-Jones nucleus revealed that the interior is FCC, but the surface structure seemed similar to base centered cubic (BCC) rather than to FCC or liquid [18].

Apparently the melt (probably solutions as well) close to a growing surface may have unexpected structures that may have a significant influence on nucleation and growth rates. Hence it is important to characterize the crystal surface in detail. First we define the neighbourhood $\Omega(i)$ of a growth unit i. For lattice systems this is straightforward, for models with continuous particle co-ordinates this is far from trivial. Several parameters are in use to characterize $\Omega(i)$, e.g. the co-ordination number $Z(i)$, the number of neighbours, and $\bar{r}(i)$, the average distance to these neighbours.

4. Neighbourhood of a growth unit

The neighbourhood $\Omega(i)$ of growth unit i is the set of neighbours of i. A definition of $\Omega(i)$ should be applicable to any configuration that can occur in a system. In obvious cases the classification by this definition should be the same as by common sense. Good algorithms contain as little adjustable parameters as possible. Preferably the co-ordination number $Z(i)$, the average neighbour distance

$\bar{r}(i)$ and the set $\Omega(i)$ vary slowly during a simulation. Of course changes at crystal growth time scales are unavoidable.

Most straightforward is the cut-off definition, where the neighbours are the growth units within the sphere with the cut-off radius r_{co} around i. This method is conceptually and computationally simple. But an obvious choice for r_{co} is available only for the rare cases, e.g. for low-temperature and hard-sphere crystals or granular matter, where the first and further neighbours are clearly separated in distance. But for a two-phase system a universal choice is more difficult, as the two phases have different neighbour distances. Especially in the interfacial region, the value chosen for r_{co} may strongly influence $\Omega(i)$ and all order parameters.

A second method is to define $\Omega(i)$ as the collection of the Z growth units that are closest to i. This definition eliminates fluctuations of the co-ordination number. An obvious choice for Z in crystal phases is the number of nearest neighbours in the average structure, e.g. $Z = 12$ for FCC and HCP. Due to temperature-induced oscillations the first and second nearest neighbours of i may mix. For BCC this is important already at relatively low-temperature, and often $Z = 14$ leads to a more constant set $\Omega(i)$ than $Z = 8$. For liquids no value of Z singles out a nearly constant set $\Omega(i)$. Note that with this method the average neighbour distance $\bar{r}(i)$ fluctuates, and that the best value for Z is different for different phases.

The third method is the Voronoi method. The Voronoi cell of growth unit i is the polyhedral region of space that is closer to i than to any other particle. Then $\Omega(i)$ is the set of growth units j that share one face of their Voronoi cell with the Voronoi cell of i. The Voronoi method is parameter free. This property makes it especially useful for the two-phase and interface systems. There are fluctuations in $Z(i)$, $\bar{r}(i)$ and $\Omega(i)$.

Summarizing, with all three definitions some 'borderline' particles will jump out of and into $\Omega(i)$, unless the first peak of the pair correlation function is completely separated from the other peaks. This implies an intrinsic variation in $\Omega(i)$. As a consequence multi-particle properties like bond angles can fluctuate strongly, even when the variance of $Z(i)$ and $\bar{r}(i)$ is only modest. The effect of these fluctuations can be reduced when borderline neighbours get a small weight in determining neighbourhood properties. Therefore we ascribe a neighbour weight $C(i,j)$ to each neighbour j of the central growth unit i, satisfying

$$\sum_{j\neq i} C(i,j) = 1. \tag{3}$$

In the first approximation $C(i,j)$ is positive and zero, respectively, for a particle j which is inside and outside $\Omega(i)$. The methods discussed so far correspond to $C(i,j) = 1/Z(i)$ for $j \in \Omega(i)$, and $C(i,j) = 0$ for $j \notin \Omega(i)$. With these choices borderline neighbours get the same weight as "permanent" neighbours.

Choices that lead to small weights $C(i,j)$ for borderline neighbours are particularly natural for the Voronoi method. Indeed, the $C(i,j)$ may be chosen proportional to the area $A(i,j)$ of the common polygon of the Voronoi cells of i and j, or proportional to the viewing angle $A(i,j)/r_{ij}^2$ from i to that polygon. We define the *neighbourhood average* $\bar{X}$ of a quantity X that depends on neighbour pairs as

$$\bar{X}(i) \equiv \sum_{j\in\Omega(i)} C(i,j)X(i,j). \tag{4}$$

An example is the average neighbour distance $\bar{r}(i)$ that can be written as

$$\bar{r}(i) = \sum_{j\in\Omega(i)} C(i,j)r_{ij}, \tag{5}$$

where $r_{ij} = |\mathbf{r}_j - \mathbf{r}_i|$ is the distance of growth units i and j. A second example is the co-ordination number that we redefine as the inverse of the average weight:

$$Z(i) \equiv \frac{1}{\bar{C}(i)} = \frac{1}{\sum_{j\in\Omega(i)} C(i,j)^2}. \tag{6}$$

Note that the co-ordination number is no longer discrete, as $C(i,j)$ is continuous. Our study showed that the Voronoi method with the weights

$$C(i,j) \div \frac{A(i,j)}{r_{ij}^2} \tag{7}$$

leads to the highest order parameter qualities. Therefore, this is our method of choice to characterize the interfacial region.

5. Characterizing local structure with atomic resolution

The key to understanding crystal growth processes at an atomic-scale lies in an accurate description of the neighbourhood of each atom. This information is comprised in the *local bond vector density*

$$\rho(i,\mathbf{r}) = \sum_{j\in\Omega(i)} C(i,j)\delta(\mathbf{r}-(\mathbf{r}_j-\mathbf{r}_i)), \tag{8}$$

where δ is the Dirac distribution. This density can be viewed as an atomic resolution microscopic image of the neighbourhood of atom i. For the purpose of recognizing a local structure, it will be sufficient to consider bond vector *directions*. Their distribution can be decomposed into spherical harmonics [19]:

$$\rho_b(i,\hat{\mathbf{r}}) \equiv \int_0^\infty \rho(i,\lambda\hat{\mathbf{r}})\,\mathrm{d}\lambda = \sum_{l=0}^{\infty}\sum_{m=-l}^{l} Q_m^l(i)\,Y_m^l(\hat{\mathbf{r}})^*. \tag{9}$$

Here $\hat{\mathbf{r}}$ is a unit vector and the $Q_m^l(i)$ are neighbourhood-averaged spherical harmonics

$$Q_m^l(i) \equiv \sum_{j\in\Omega(i)} Y_m^l(\hat{\mathbf{r}}_{ij})C(i,j) \tag{10}$$

and $\hat{\mathbf{r}}_{ij} = (\mathbf{r}_j-\mathbf{r}_i)/r_{ij}$ is the unit vector pointing from i towards j.

Rotation-invariant combinations of local bond order parameters can be used as "fingerprints" to investigate interfaces during growth and nucleation. The bipolar product

$$Q^l(i,j) \equiv \frac{4\pi}{2l+1}\sum_{m=-l}^{l} Q_m^l(i)Q_m^l(j)^* \tag{11}$$

and the tripolar product, which involves Wigner $3j$ symbols,

$$W^{l_1l_2l_3}(i,j,k) = \sum_{m_1=-l_1}^{l_1}\sum_{m_2=-l_2}^{l_2}\sum_{m_3=-l_3}^{l_3}\begin{pmatrix} l_1 & l_2 & l_3 \\ m_1 & m_2 & m_3\end{pmatrix} \times Q_{m_1}^{l_1}(i)Q_{m_2}^{l_2}(j)Q_{m_3}^{l_3}(k) \tag{12}$$

are rotation invariant. They only depend on angles between bond vectors around i, j and k.

Instantaneous values of local bond order parameters for individual atoms or for groups of atoms are used to select the best matching reference phase. To judge order parameter in this respect, we defined a *selection quality* $K_{\mathrm{sel}}(O)$ of an order parameter O that measures the fraction of wrong assignments. Probability *distributions* of order parameters can be obtained by accumulating data during some time or over a space region. They are used to decompose the measured data into contributions from different reference phases. The *decomposition quality* $K_{\mathrm{dec}}(O)$ measures the RMS difference of the estimated and the real composition of a mixed phase. In an independent paper we shall explain how these quality factors can be obtained from probability distributions $h_\alpha(O)$ for n reference phases α, e.g. $n=4$: α = FCC, HCP, BCC or liquid [20]. Both quality factors turn out to lead to roughly, but not exactly the same ordering of bond order parameters.

It is important, especially close to the melting point, to choose the optimal order parameter for the type of investigation at hand. Average values and distributions of $Q^l(i,i)$ and $W^{lll}(i,i,i)$ with $l=4$, 6 and 8 have been used to recognize HCP, HCP, BCC and liquid phases near interfaces. We have carried out a thorough investigation, involving several hundred thousands of order parameters. Our study revealed that different order parameters have to be chosen, depending on which phases we want to recognize. Distinguishing two phases we found that FCC is easy to recognize: a best $K_{\mathrm{sel}}(O)\approx 0.02$ is found when one of the two phases is FCC. On the other hand a best $K_{\mathrm{sel}}(O)\approx 0.07$ is obtained for pairs made of HCP, BCC and liquid. For four phases, the frequently used order parameters $Q^6(i,i)$ and $W^{666}(i,i,i)$ with $Z=12$ neighbours, led to $K_{\mathrm{sel}}(Q^6)=0.36$ and $K_{\mathrm{sel}}(W^{666})=0.35$, respectively. The best result, $K_{\mathrm{sel}}(W^{668})=0.27$, was obtained with $Z=11$ neighbours. When choosing Voronoi neighbourhood definitions similar values were found.

Overlapping of order parameter distributions causes the rather poor performance. The overlapping parts of the distributions, however, are different for different order parameters. Therefore

we use combinations of two or more order parameters. The best joint order parameter with Voronoi neighbourhood definitions that we found for distinguishing the four phases is $\mathbf{O} = (W^{446}, W^{668})$ with $K_{\mathrm{sel}}(\mathbf{O}) = 0.07$, for decomposition the best was $\mathbf{O} = (W^{61212}, W^{668})$ with $K_{\mathrm{dec}}(\mathbf{O}) = 0.21$. We used these order parameters to study interface structures.

In Fig. 1 phase weight profiles $w_\alpha(z - z_{\mathrm{int}})$ are shown for the (0 0 1) crystal-melt surface of an FCC Lennard–Jones crystal at the normal ($P =$ 1 atm) melting point $T_{\mathrm{m}} = 70.6$ K. Here $z - z_{\mathrm{int}}$ is a distance into the liquid and z_{int} is the position where the solid and the liquid weights are equal. Data of the (equivalent) upper and lower surface of the crystal slab are superimposed to give an impression of the accuracy that we have achieved. Similar profiles were obtained for (1 1 1), (1 1 0) and (1 1 2) orientations.

These 8000-particle systems were constructed by connecting an equilibrated FCC crystal to a liquid with the proper lateral dimensions. The total length of the combined system was carefully adjusted until at the two-phase equilibrium, both the solid and the liquid phase were about 11 nm thick. In this system NVT simulations were carried out.

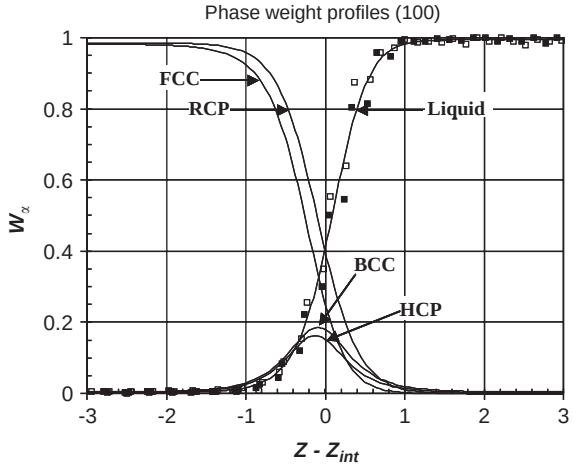

Fig. 1. Example of decomposed phase weight profiles for a (1 0 0) interface. Lines are fits through measured phase weights, □ and ■ are liquid weight values found at the upper and lower side of the crystal slab.

In order to have optimal resolution and minimal noise of the profiles, we divided the system into slices that were as thin as possible while still containing equivalent sets of atoms in the crystal and in the liquid phase. In the crystal slab each slice had a thickness of $d_{hkl}/2$ and extended from the middle of a crystal layer to midway in between two layers. This procedure could be extended to several slices into the interface region. In the bulk liquid a constant slice thickness was chosen, close to that of the last recognizable interface slice. In this way, the system was divided into 100–150 slices parallel to the surface. For each slice a histogram for $\mathbf{O} = \left(W^{468}, W^{668}\right)$ was obtained from 100 measurements with 1000 MC steps per particle in between, and fitted to the reference histograms to obtain four phase weights w_{FCC}, w_{HCP}, w_{BCC} and w_{liq} in that slice. During the equilibration period several crystal layers may have grown or molten. For the (1 1 1) surface we found a few HCP layers near the surface, due to random stacking of hexagonal layers (RCP phase) for this growth direction. Therefore the total close-packed fraction $w_{\mathrm{RCP}} \equiv w_{\mathrm{FCC}} + w_{\mathrm{HCP}}$ is more meaningful than w_{FCC} and w_{HCP} separately.

Due to our optimisation of order parameters and reference histograms, the solid and the liquid regions are well localized, and contain very little (spurious) fractions of other phases. In earlier studies the liquid phase often seemed to contain significant BCC or HCP structure.

In order to characterize the measured profiles quantitatively, we fitted them to the form

$$w(z) = A + B\tanh(C\tilde{z}(z - z_{\mathrm{int}})) \tag{13}$$

for FCC and liquid fractions and

$$w(z) = A + B\cosh(C\tilde{z}(z - z_{\mathrm{int}})) \tag{14}$$

for HCP and BCC fractions. The function

$$\tilde{z}(u) = u + \sqrt{D^2u^2 + 1} - 1 \tag{15}$$

was introduced to capture asymmetric profiles. Using the five parameters A, B, C, D and z_{int}, all profiles were fitted for 3 nm on both sides of the surface with a precision of 1% or better. From these, we get the physical parameters, e.g. the effective interface thickness of the surface phases

$\alpha = \mathrm{BCC}$ and $\alpha = \mathrm{HCP}$ is

$$\Delta_\alpha = \int_{-\infty}^{\infty} w_\alpha(z)\,\mathrm{d}z, \tag{16}$$

whereas the interface extension at the solid and liquid sides are estimated by

$$\Delta_s = \int_{-\infty}^{z_{\mathrm{int}}} (1 - w_{\mathrm{FCC}}(z))\,\mathrm{d}z + \sum_{\alpha \neq \mathrm{FCC}} \int_{-\infty}^{z_{\mathrm{int}}} w_\alpha(z)\,\mathrm{d}z, \tag{17}$$

$$\Delta_l = \int_{z_{\mathrm{int}}}^{\infty} (1 - w_{\mathrm{liq}}(z))\,\mathrm{d}z + \sum_{\alpha \neq \mathrm{liq}} \int_{z_{\mathrm{int}}}^{\infty} w_\alpha(z)\,\mathrm{d}z \tag{18}$$

and an analogous expression is used for the solid side. The fitting results are given in Table 1.

An important observation is that nowhere the BCC structure is dominant. The largest BCC weight is about 20%, but this occurs in the middle of the interface region where similar weights are ascribed to at least one of the three other phases. We also found a much larger BCC weight if the HCP reference phase was artificially omitted, which led us to the conclusion that the reported BCC-structure at the surface of a nucleus [18] is not found at a flat interface, and its observation might be an artefact of omitting the HCP reference phase.

What came to us as a surprise is that the phase profiles are so similar for all four orientations, i.e. the profile depth is the same in nm, though quite different in terms of the number of crystal layers involved. The small differences seem insufficient to explain the observed anisotropy of the growth rate, in particular, the rapid growth of the (1 0 0) orientation. Presumably new order parameters have to be developed that are more sensitive to layering of the liquid phase, as this seems to differ most among the four orientations that we studied.

Table 1
Interface characteristics

	(1 1 1)	(1 0 0)	(1 1 0)	(1 1 2)
$\Delta_s + \Delta_l$ (nm)	0.710	0.919	0.809	0.849
Δ_l/Δ_s	0.800	0.807	0.716	0.784
$w_{\mathrm{BCC,max}}$	0.191	0.185	0.195	0.175
Δ_{BCC} (nm)	0.179	0.222	0.207	0.202
$w_{\mathrm{HCP,max}}$	—	0.163	0.183	0.163
Δ_{HCP} (nm)	—	0.182	0.176	0.162

A further application of bond order parameters is to test whether two particles have a similar environment, by checking whether the *connectivity factor*

$$\gamma^l(i,j) \equiv Q^l(i,j)/\sqrt{Q^l(i,i)Q^l(j,j)} \tag{19}$$

for the two atoms exceeds a predetermined threshold. This allows one to define clusters and to study the size and the shape of a nucleus.

6. Structure assessment by ensemble of force networks

The structure of condensed matter is, to a large extent, determined by short-range intermolecular repulsive forces. Already in the early days of liquid-phase statistical mechanics one concluded that many properties of liquids could be understood using a hard sphere model with an appropriate hard sphere radius. The hard sphere model possesses a first-order liquid–solid phase transition. Also, when I asked Professor Hartman 25 years ago, which interactions should be taken into account in a Hartman–Perdok morphology analysis, he gave me the puzzling advice to consider only short-range *repulsive* interactions.

In line with this philosophy, the ensemble of force networks (EFN) method [21,22] describes structural properties in terms of short-range repulsive forces. In our view this method is very promising for the further development of our understanding of liquid–solid transformation, i.e. crystal growth from the melt.

The EFN method has been developed recently to describe the stability of granular material. The elementary particles of granular matter are small, but macroscopic grains which dominantly interact with a very short-range repulsive interaction (almost hard spheres or other hard bodies). Thus, for one set of centre of mass positions, many different force configurations are conceivable if a small

dispersion in size or shape of the grains is taken into account. The set of all repulsive force configurations that leave a given configuration of particles in rest (i.e. zero total force $\mathbf{F}(i)$ on each particle with a given value for the average strength $\langle f_{ij} \rangle$ of the pair forces) is called the EFN. Note that the repulsive forces in each member of the ensemble may be, and in general are, quite different from the actual interparticle forces.

The merits of the EFN for crystal growth will be discussed in the lecture by Vlugt. Here, we only want to stipulate that so far in the EFN, neighbours with a possibly non-zero repulsive interaction are selected with a cut-off criterion. A natural generalization of the EFN would be to introduce the Voronoi neighbourhood definition. This might open a window to use the EFN as a tool to characterize the structure of a crystal–melt interface.

7. Conclusion

In this lecture an overview has been given of the state of the art in using local bond order parameters to understand surface structures. It has been shown that different approaches are necessary depending on the problem one is considering. Different groups have worked on these problems and several new and efficient methods have been developed.

An important application of bond order parameters is to help bridging the gaps between ab initio calculations, molecular-scale simulations and phase field models of crystal growth, e.g. the orientation-dependent growth rate and interface profiles, that we have discussed here might be used to estimate the (possibly anisotropic) capillarity lengths and kinetic coefficients that are input parameters for phase field descriptions. Alternatively, the determination of relevant order parameters, may provide important and representative atom configurations for given phases and interfaces. Ab initio calculations on such configurations could help to develop and parameterize relevant interaction models that lead to tractable MC or MD simulations.

Acknowledgement

This paper is based on the support and the dedicated work of our colleagues Fiona Yarrow, Edzer Huitema and Margot Vlot.

References

[1] W. Kossel, Nachr. Ges. Wiss. Göttingen (1927) 135.
[2] I. Stranski, R. Kaischew, Z. Phys. Chem. B 26 (1934) 100.
[3] W.K. Burton, N. Cabrera, F.C. Frank, Trans. Roy. Soc. A 243 (1951) 299.
[4] J.M. Kosterlitz, D.J. Thouless, J. Phys. Chem. C 6 (1973) 1181.
[5] J.P.v.d. Eerden, in: D.T.J. Hurle (Ed.), Handbook of Crystal Growth 1a, North-Holland, Amsterdam, 1993, p. 307.
[6] S.X.M. Boerrigter, Thesis: Modeling of Crystal Morphology: Growth Simulation on Facets in Arbitrary Orientations, 2002, Dept. of Solid State Chemistry, Nijmegen.
[7] S.X.M. Boerrigter, G.P.H. Josten, J. van de Streek, J. Los, H.M. Cuppen, P. Bennema, H. Meekes, J. Phys. Chem. A 108 (2004) 5894.
[8] E. Burke, J.Q. Broughton, J. Chem. Phys. 89 (1988) 1030.
[9] J.Q. Broughton, G.H. Gilmer, J. Chem. Phys. 79 (1983) 5095.
[10] J.Q. Broughton, G.H. Gilmer, J. Chem. Phys. 79 (1983) 5105.
[11] J.Q. Broughton, G.H. Gilmer, J. Chem. Phys. 79 (1983) 5119.
[12] J.Q. Broughton, G.H. Gilmer, J. Chem. Phys. 84 (1986) 5741.
[13] J.Q. Broughton, G.H. Gilmer, J. Chem. Phys. 84 (1986) 5749.
[14] J.Q. Broughton, G.H. Gilmer, J. Chem. Phys. 84 (1986) 5759.
[15] J.S.v. Duijneveldt, D. Frenkel, J. Chem. Phys. 99 (1992) 4655.
[16] P.R. ten Wolde, M.J. Ruiz-Montero, D. Frenkel, J. Chem. Phys. 104 (1996) 9932.
[17] H.E.A. Huitema, J.P.J.M.v.d. Eerden, J.J.M. Janssen, H. Human, Phys. Rev. B 62 (22) (2000) 14690.
[18] P.R. ten Wolde, M.J. Ruiz-Montero, D. Frenkel, Phys. Rev. Lett. 75 (1995) 2714.
[19] D.A. Varshalovich, A.N. Moskalev, V.K. Khersonskii, Quantum Theory of Angular Momentum, World Scientific, Singapore, 1988, pp. 130–169.
[20] J. Makkinje, Thesis: Local Order Parameters for Crystal Growth, 2005, Dpt. Condensed Matter and Interfaces, Utrecht University.
[21] J.H. Snoeijer, T.J.H. Vlugt, M. van Hecke, W. van Saarloos, Phys. Rev. Lett. 92 (5) (2004) 054302.
[22] J.H. Snoeijer, T.J.H. Vlugt, W.G. Ellenbroek, M. van Hecke, J.M.J. van Leeuwen, Phys. Rev. E, in press (December 2005).